Gold and Silver Complexes with the Ferrocenyl Phosphine $FcCH_2PPh_2$ [Fc = (η^5-C_5H_5)Fe(η^5-C_5H_4)]

Eva M. Barranco, Olga Crespo, M. Concepción Gimeno, and Antonio Laguna*

Departamento de Química Inorgánica, Instituto de Ciencia de Materiales de Aragón, Universidad de Zaragoza-CSIC, E-50009 Zaragoza, Spain

Peter G. Jones and Birte Ahrens

Institut für Anorganische und Analytische Chemie der Technischen Universität, Postfach 3329, D-38023 Braunschweig, Germany

Received May 17, 1999

Linear gold(I) and silver(I) complexes with the ferrocenyl phosphine $FcCH_2PPh_2$ [Fc = (η^5-C_5H_5)Fe(η^5-C_5H_4)] of the types [AuR(PPh_2CH_2Fc)], [M(PPh_3)(PPh_2CH_2Fc)]OTf, and [M(PPh_2CH_2Fc)$_2$]OTf (M = Au, Ag) have been obtained. Three-coordinate gold(I) and silver(I) derivatives of the types [AuCl(PPh_2CH_2Fc)$_2$] and [M(PPh_2CH_2Fc)$_3$]X (M = Au, X = ClO_4; M = Ag, X = OTf) have been obtained from the corresponding gold and silver precursors in the appropriate molar ratio, although some of them are involved in equilibria in solution. The crystal structures of [AuR(PPh_2CH_2Fc)] (R = Cl, C_6F_5), [AuL(PPh_2CH_2Fc)]OTf (L = PPh_3, $FcCH_2PPh_2$), [Au(C_6F_5)$_3$(PPh_2CH_2Fc)], and [Ag(PPh_2CH_2Fc)$_3$]OTf have been determined by X-ray diffraction studies.

Introduction

Phosphine ligands containing ferrocene moieties currently attract a great deal of interest, as is shown by the large number of transition metal complexes described for the chelating ligand 1,1′-bis(diphenylphosphino)ferrocene (dppf).[1] Much attention has also been paid to chiral ferrocenyl phosphines in asymmetric catalysis.[2,3] In all of these ligands the phosphine moiety is linked directly by a P−C bond to the cyclopentadienyl ring of the ferrocene. However, examples of ferrocenyl phosphines containing a carbon spacer between the cyclopentadienyl ring and the phosphorus atom are rare. Although the synthesis of the first (ferrocenylmethyl)phosphine was reported as early as 1963,[4,5] only recently has the 1,1′-bis(diphenylphosphinomethyl)-ferrocene been synthesized[6] or the reactivity of $FcCH_2P(CH_2OH)_2$ (leading to various ferrocene-derived phosphines or metal complexes) studied.[7−10]

As part of our studies in ferrocene derivatives as ligands in gold chemistry,[11] we report here the synthesis of several gold and silver complexes with the (ferrocenylmethyl)phosphine $FcCH_2PPh_2$, whose coordination chemistry has not yet been studied. Two- and three-coordinate gold and silver complexes have been prepared. Cyclic voltammetry shows one-electron reversible oxidation based on the ferrocene moiety.

Results and Discussion

Synthesis. The reaction of $FcCH_2PPh_2$ with 1 equiv of [AuX(tht)] (tht = tetrahydrothiophene) in dichloromethane gives orange solids of the neutral complexes [AuR(PPh_2CH_2Fc)] (R = Cl, **1**; C_6F_5, **2**) (see Scheme 1). These are air- and moisture-stable and are nonconducting in acetone solutions. Their IR spectra show the vibration ν(Au−Cl) at 336 (m) cm^{-1} (**1**) and the bands arising at the pentafluorophenyl group bonded to gold(I) at 1505 (vs), 954 (s), and 790 (m) cm^{-1} (**2**).

The ^{1}H NMR spectra show two multiplets for the α and β protons of the substituted cyclopentadienyl group, a singlet for the protons of the unsubstituted Cp, and a doublet for the protons of the methylene group, which are coupled with the phosphorus atom. The ^{19}F NMR spectrum of **2** presents three resonances for the three different fluorines of the pentafluorophenyl group.

(1) Gan, K. S.; Hor, T. S. A. In *Ferrocenes. Homogeneous Catalysis, Organic Synthesis and Materials Science*; Togni, A., Hayashi, T., Eds.; VCH: Weinheim, 1995; Chapter 1 and references therein.
(2) Hayashi, T. *Ferrocenes.* In *Homogeneous Catalysis, Organic Synthesis and Materials Science*; Togni, A., Hayashi, T., Eds.; VCH: Weinheim, 1995; Chapter 2 and referencess therein.
(3) Togni, A. In *Metallocenes*; Togni, A., Halterman, R. L., Eds.; VCH: Weinheim, 1998; Vol. 2, Chapter 11.
(4) Pauson, P. L.; Watts, W. E. *J. Chem. Soc.* **1963**, 2990.
(5) Marr, G.; White, T. M. *J. Chem. Soc., Perkin Trans. 1* **1973**, 1955.
(6) Yamamoto, Y.; Tanese, T.; Mori, I.; Nakamura, Y. *J. Chem. Soc., Dalton Trans.* **1994**, 3191.
(7) Goodwin, N. J.; Henderson, W.; Sarfo, J. K. *Chem. Commun. (Cambridge)* **1996**, 1551.
(8) Goodwin, N. J.; Henderson, W.; Nicholson, B. K.; Sarfo, J. K.; Fawcett, J.; Russell, D. R. *J. Chem. Soc., Dalton Trans.* **1997**, 4377.
(9) Goodwin, N. J.; Henderson, W.; Nicholson, B. K. *Chem. Commun. (Cambridge)* **1997**, 31.
(10) Goodwin, N. J.; Henderson, W. *Polyhedron* **1998**, *17*, 4071.
(11) (a) Gimeno, M. C.; Laguna, A.; Sarroca, C.; Jones, P. G. *Inorg. Chem.* **1993**, *32*, 5926. (b) Gimeno, M. C.; Laguna, A.; Sarroca, C.; Jones, P. G. *J. Chem Soc., Dalton Trans.* **1995**, 1473. (c) Gimeno, M. C.; Jones, P. G.; Laguna, A.; Sarroca, C. *J. Chem Soc., Dalton Trans.* **1995**, 3563. (d) Canales, F.; Gimeno, M. C.; Laguna, A.; Jones, P. G. *J. Am. Chem. Soc.* **1996**, *118*, 4839. (e) Canales, F.; Gimeno, M. C.; Laguna, A.; Jones, P. G. *Organometallics* **1996**, *15*, 3412. (f) Gimeno, M. C.; Jones, P. G.; Laguna, A.; Sarroca, C. *J. Chem Soc., Dalton Trans.* **1998**, 1277. (g) Crespo, O.; Gimeno, M. C.; Jones, P. G.; Laguna, A.; Sarroca, C. *Chem. Commun. (Cambridge)* **1998**, 1481. (h) Gimeno, M. C.; Jones, P. G.; Laguna, A.; Sarroca, C. *Polyhedron* **1998**, *17*, 3681. (i) Gimeno, M. C.; Jones, P. G.; Laguna, A.; Sarroca, C.; Calhorda, M. J.; Veiros, L. F. *Chem.—Eur. J.* **1998**, *4*, 2308. (j) Barranco, E. M.; Gimeno, M. C.; Laguna, A.; Villacampa, M. D.; Jones, P. G. *Inorg. Chem.* **1999**, *38*, 702.

10.1021/ic9905446 CCC: $19.00
Published on Web 01/29/2000

Scheme 1[a]

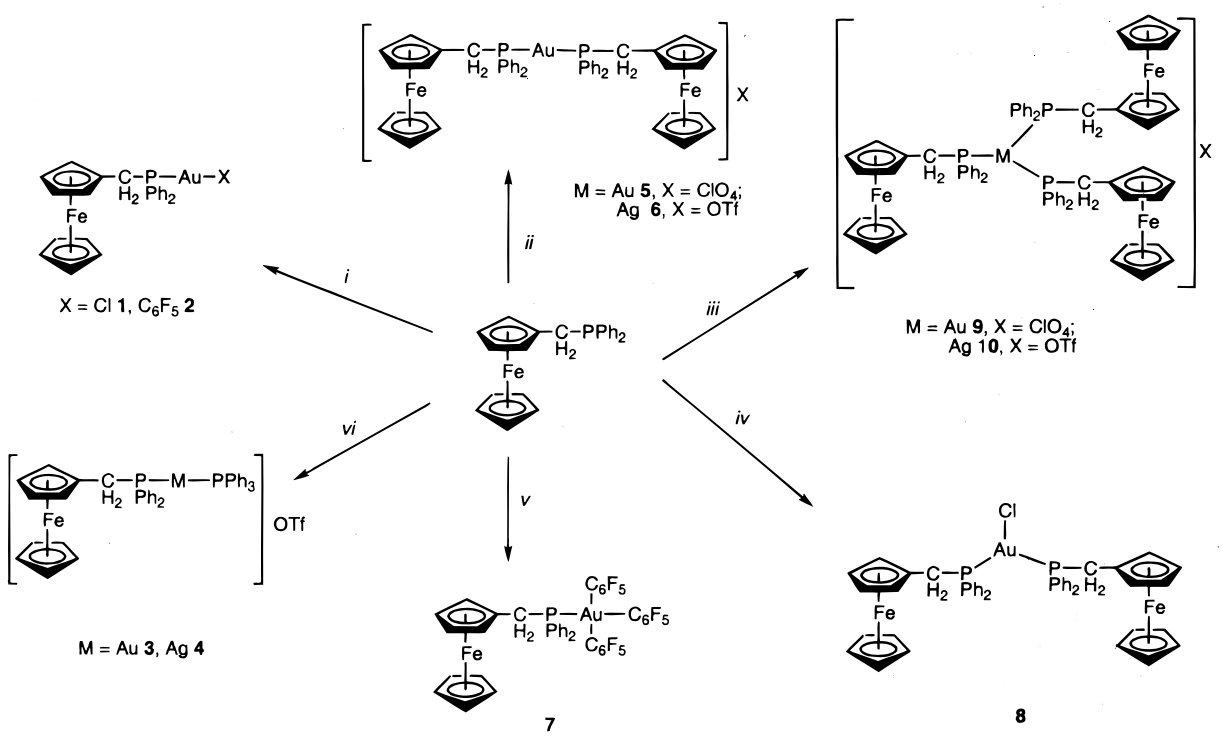

[a] (i) [AuCl(tht)] or [Au(C_6F_5)(tht)], (ii) $^1/_2$[Au(tht)$_2$]ClO_4 or Ag(OTf), (iii) $^1/_3$[Au(tht)$_2$]ClO_4 or Ag(OTf), (iv) $^1/_2$[AuCl(tht)], (v) [Au(C_6F_5)$_3$(tht)], (vi) [Au(OTf)(PPh_3)] or [Ag(OTf)(PPh_3)].

In the positive liquid secondary-ion mass spectra (LSIMS) the molecular peaks appear at m/z = 616 (**1**, 100%) and 748 (**2**, 100%). Other fragmentation peaks $[M - X]^+$ or association peaks $[M + Au]^+$ and $[2M - X]^+$ are present in both spectra.

The treatment of $FcCH_2PPh_2$ with [M(OTf)PPh_3] in dichloromethane and in equal molar ratio leads to the cationic complexes [M(PPh_3)(PPh_2CH_2Fc)]OTf (M = Au, **3**; Ag, **4**) in high yield. Complexes **3** and **4** are air- and moisture-stable yellow solids that behave as 1:1 electrolytes in acetone solutions. Their IR spectra show, apart from the bands arising from the phosphine ligands, those of the trifluoromethanesulfonate at 1265 (vs, br) [$\nu_{as}(SO_3)$], 1223 (s) [$\nu_s(CF_3)$], 1150 (s) [$\nu_{as}(CF_3)$], and 1023 (s) [$\nu_s(SO_3)$] cm^{-1}.

The ^{1}H NMR spectrum of complex **3** shows, apart from the multiplet from the phenyl protons, the signals of the ferrocenyl unit as one multiplet for the unsubstituted Cp ring, two multiplets for the α and β protons of the substituted cyclopentadienyl ring, and one multiplet for the protons of the methylene group. Variable-temperature NMR spectra (CD_2Cl_2) show no variation of the appearance of the signals with the temperature up to −80 °C. The $^{31}P\{^1H\}$ NMR spectrum shows two resonances at 44.0 and 44.8 ppm for the two different phosphorus environments. Variable-temperature studies also show no variation of the signals. Usually in this type of complex an AB system appears, which in this case is not observed owing to fast ligand exchange in solution even at −80 °C. Complex **4** shows five multiplets with a 25:5:2:2:2 ratio for the phenyl protons and ferrocene moiety. The $^{31}P\{^1H\}$ NMR spectrum at room temperature consists of a broad signal that sharpens into an AB system coupled to both silver nuclei ^{107}Ag and ^{109}Ag. The simulated spectrum agrees with the experimental.

In the positive liquid secondary-ion mass spectra (LSIMS), the cationic molecular peaks appear at m/z = 843 (**3**, 100%) and 753 (**4**, 46%), respectively.

We have also prepared homoleptic cationic gold(I) or silver(I) complexes of the type [M(PPh_2CH_2Fc)$_2$]X (M = Au, X = ClO_4, **5**; M = Ag, X = OTf, **6**) starting from [Au(tht)$_2$]ClO_4 or AgOTf in dichloromethane or diethyl ether, respectively. They are air- and moisture-stable yellow solids that behave as 1:1 electrolytes in acetone solutions. Their IR spectra show the bands of the ferrocenyl phosphine ligand and of the anion OTf or ClO_4 [1100 (vs, br) and 620 (s) cm^{-1}]. The ^{1}H NMR spectra show the typical pattern of a monosubstituted ferrocene and two multiplets for the methylene and phenyl protons. The $^{31}P\{^1H\}$ NMR spectra consist of a singlet for the gold complex and a broad signal for the silver derivative; the latter splits into two doublets by coupling with the two silver nuclei ^{107}Ag and ^{109}Ag. In the positive secondary-ion mass spectra the molecular peaks appear at m/z = 1064 (**5**, 3%) and 1026 (**6**, 3%), although with low intensity; in both cases the most intense peaks are the cationic molecular peaks that appear at m/z = 965 and 875, respectively.

The gold(III) derivative, [Au(C_6F_5)$_3$(PPh_2CH_2Fc)] (**7**), has been prepared by reaction of the phosphine with [Au(C_6F_5)$_3$(OEt_2)] in a 1:1 molar ratio. Complex **7** is an air- and moisture-stable solid that behaves as nonconductor in acetone solutions. Its IR spectrum shows the typical pattern for an "Au(C_6F_5)$_3$" unit, with bands at 970 (s), 803 (s), and 795 (m) cm^{-1}, and the bands from the ferrocenyl phosphine.

The ^{1}H NMR spectrum shows a doublet for the methylene protons coupled to the phosphorus atom, two multiplets for the α and β protons of the C_5H_4 ring, and a singlet for the C_5H_5 ring. The $^{31}P\{^1H\}$ NMR spectrum consists of a multiplet as a result of the coupling of the phosphorus atoms with the fluorine nuclei. The ^{19}F NMR spectrum shows six resonances corresponding to two types of pentafluorophenyl groups in a 2:1 ratio, corresponding to the ortho, meta, and para fluorines of each C_6F_5 unit.

Scheme 2

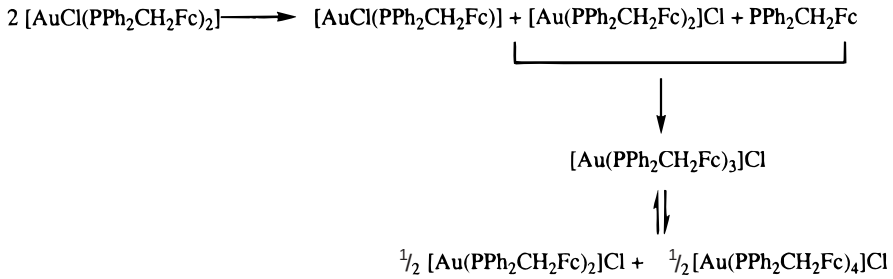

The LSIMS mass spectrum shows the molecular peak at m/z = 1082 (100%) and other fragmentation peaks at m/z = 748 ($[Au(C_6F_5)(PPh_2CH_2Fc)]^+$), 581 ($[Au(PPh_2CH_2Fc)]^+$), and 384 ($PPh_2CH_2Fc^+$).

The three-coordinate gold complex $[AuCl(PPh_2CH_2Fc)_2]$ (**8**) has been obtained by reaction of [AuCl(tht)] and 2 equiv of PPh_2CH_2Fc.

The ^1H NMR spectrum of complex **8** at room temperature in dichloromethane shows three multiplets in a 2:2:5 ratio for the ferrocene protons and a doublet for the methylene protons. In the $^{31}P\{^1H\}$ NMR spectrum, a broad singlet at 33.8 appears because of the equivalence of the phosphorus atoms. The variable-temperature ^1H NMR spectra show broadening of the signals in the range −20 to −40 °C, and below −60 °C five signals appear in the ferrocene region. The $^{31}P\{^1H\}$ NMR spectrum also shows broadening of the signal; at −20 °C two broad signals appear, from −40 to −60 °C two singlets are present at 32.4 and 42.3 ppm, and at −80 °C two more small resonances appear at 38.5 and 28.2 ppm. The two main resonances possess chemical shifts close to those in the complexes $[Au(PPh_2CH_2Fc)_2]ClO_4$ and $[AuCl(PPh_2CH_2Fc)]$. According to these data we propose that there is an equilibrium between three- and two-coordinate species such that at room temperature the three-coordinate complex is present and at low temperature a reorganization process takes place (Scheme 2). If this process takes place, the presence of free phosphine should be observed, but we do not see this in the NMR time scale; therefore, we propose that the free phosphine would react immediately with the $[AuP_2]^+$ complex to give the three-coordinate species. The latter, as we propose below, is in equilibrium with the linear and four-coordinate species. This explain the four resonances present that are only seen at −80 °C. To corroborate this we have also carried out variable-temperature studies of a sample prepared "in situ" from 1 equiv of [AuCl(tht)] and 2 equiv of the phosphine. The spectra at different temperatures are similar, but now below −60 °C the four signals can be observed and those at 28.2 (AuP_4^+) and 38.3 (AuP_3^+) ppm with more intensity.

The LSIMS mass spectrum shows the molecular peak at m/z = 1001, although with very low intensity (3%). The most intense peak appears at m/z = 965 and corresponds to the loss of the chlorine ligand.

We have also carried out the reactions of 3 equiv of the phosphine PPh_2CH_2Fc with $[Au(tht)_2]ClO_4$ or AgOTf, leading to the three-coordinate compounds $[Au(PPh_2CH_2Fc)_3]ClO_4$ (**9**) and $[Ag(PPh_2CH_2Fc)_3]OTf$ (**10**). The ^1H NMR spectra of both complexes show multiplets for the methylene, substituted and unsubstituted Cp, and phenyl protons, whereas the $^{31}P\{^1H\}$ spectra show broad signals at chemical shifts different from those observed for complexes **5** or **6**. In the LSIMS mass spectra the molecular peak appears only for complex **10** at m/z = 1349 (2%).

Low-temperature $^{31}P\{^1H\}$ NMR spectral studies have been carried out for both complexes. For complex **9** the initial resonance at 41.7 splits into three with different intensities at 43.8, 38.3, and 28.2 ppm. We also propose an equilibrium between the different species, $[Au(PPh_2CH_2Fc)_2]^+$, $[Au(PPh_2CH_2Fc)_3]^+$, and $[Au(PPh_2CH_2Fc)_4]^+$, respectively, in a manner similar to that reported for other tertiary phosphines (eq 1).[12] Complex **10** shows two doublets in the ^{31}P spectrum because of the coupling of the equivalent phosphorus with both silver nuclei.

$$2[Au(PPh_2CH_2Fc)_3]ClO_4 \rightleftharpoons [Au(PPh_2CH_2Fc)_2]ClO_4 + [Au(PPh_2CH_2Fc)_4]ClO_4 \quad (1)$$

Crystal Structure Determinations. Crystal Structures of [AuR(PPh$_2$CH$_2$Fc)] (R = Cl (1), C$_6$F$_5$ (2)). The crystal structures of the neutral complexes $[AuR(PPh_2CH_2Fc)]$ (R = Cl (**1**), C_6F_5 (**2**)) have been determined by X-ray diffraction studies. Figures 1a and 2 show their molecular structures, and a selection of bond lengths and angles are presented in Tables 1 and 2. In these complexes the gold atoms exhibit a very regular linear geometry, with P−Au−Cl and P−Au−C angles of 176.01(7)° and 174.3(2)°, respectively. For complex **1** the Au−Cl distance, 2.3014(18) Å, is similar to those found in complexes with ferrocenyl phosphines such as $[Au_2Cl_2(\mu\text{-dppf})]$ (dppf = 1,1′-bis(diphenylphosphino)ferrocene) (two independent determinations: 2.2815(13), 2.273−2.300 Å)[13,14] or $[AuCl(PFc_2Ph)]$ (2.289(2) Å).[15] The shortest gold−gold distance in the lattice is 5.388 Å, which excludes the possibility of any bonding interaction between gold atoms. However, there are unusually short H···Au contacts: H11···Au ($1-x$, $-y$, $1-z$) 2.73, H33···Au (x, $0.5-y$, $-0.5+z$) 2.76 Å, and also three weak intermolecular C−H···Cl contacts (H···Cl 2.88−2.91 Å) of acceptable linearity that may correspond to weak hydrogen bonds. The secondary contacts are shown in Figure 1b.

The Au−C(11) distance in **2**, 2.070(5) Å, compares well with those obtained for other gold(I) complexes, such as $[Au(C_6F_5)(PPh_3)]$ (2.07(2) Å)[16] or the ferrocene derivative $[Au_2(\mu\text{-dppf})(C_{16}H_9)_2]$ (2.061(8) Å).[17] Again the complex does not display aurophilic interactions (the shortest gold−gold distance is 5.560 Å); but in the lattice there are contacts F2···F2 of 2.858 Å and F···H34 of 2.55 and 2.60 Å.

(12) Gimeno, M. C.; Laguna, A. *Chem. Rev.* **1997**, *97*, 511 and references therein.
(13) Hill, D. T.; Girard, G. R.; McCabe, F. L.; Johnson, R. K.; Stupik, P. D.; Zhang, J. H.; Reiff, W. M.; Eggleston, D. S. *Inorg. Chem.* **1989**, *28*, 3529.
(14) Canales, F.; Gimeno, M. C.; Jones, P. G.; Laguna, A.; Sarroca, C. *Inorg. Chem.* **1997**, *36*, 5206.
(15) Jones, P. G.; Freire Erdbrügger, C.; Hohbein, R.; Schwarzmann, E. *Acta Crystallogr.* **1988**, *C44*, 1302.
(16) Baker, R. W.; Pauling, J. P. *J. Chem. Soc. Dalton Trans.* **1972**, 2264.
(17) Yam, V. W. W.; Choi, S. W. K.; Cheung, K. K. *J. Chem Soc., Dalton Trans.* **1996**, 3411.

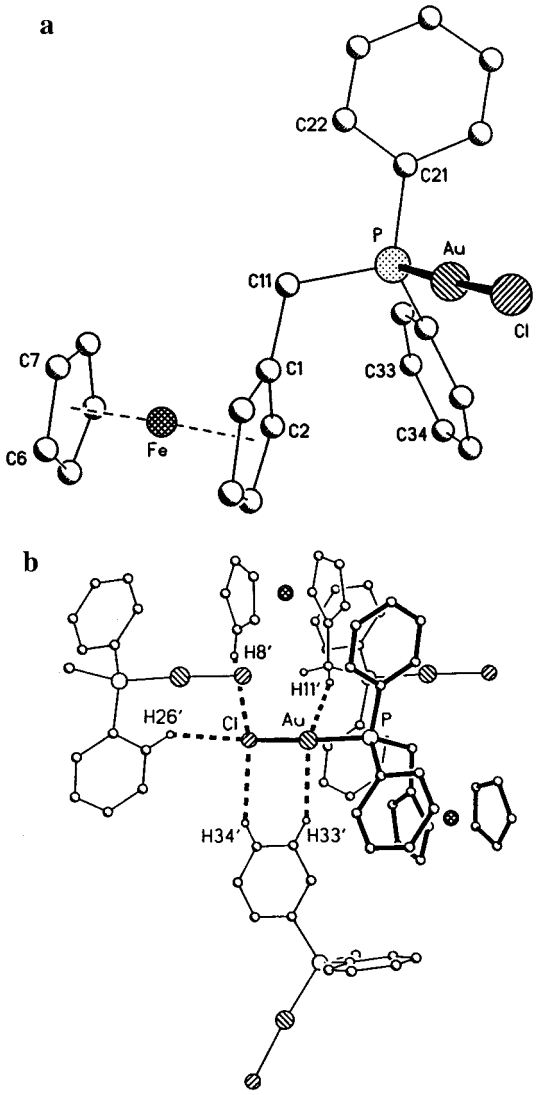

Figure 1. (a) Structure of complex **1** in the crystal with the atom-numbering scheme. The H atoms are omitted for clarity. (b) Environment of the molecule of **1**. The parent molecule is drawn with thick bonds, and secondary contacts (see text) are drawn as broken bonds. Only H atoms involved in secondary contacts are shown. Ferrocene moieties of peripheral molecules are omitted for clarity.

Table 1. Selected Bond Lengths (Å) and Angles (deg) for Complex **1**

Au−P	2.2366(18)	P−C(21)	1.821(7)
Au−Cl	2.3014(18)	P−C(11)	1.843(6)
P−C(31)	1.807(7)	C(1)−C(11)	1.508(9)
P−Au−Cl	176.01(7)	C(9)−C(10)−Fe	70.4(4)
C(31)−P−C(21)	108.5(3)	C(1)−C(11)−P	111.9(4)
C(31)−P−C(11)	100.4(3)	C(26)−C(21)−P	118.2(5)
C(21)−P−C(11)	106.6(3)	C(22)−C(21)−P	122.8(5)
C(31)−P−Au	116.2(2)	C(36)−C(31)−P	119.7(5)
C(21)−P−Au	110.3(2)	C(32)−C(31)−P	118.6(5)
C(11)−P−Au	114.2(2)		

The Au−P distances are 2.2366(18) Å in **1** and 2.284(2) Å in **2**; the difference may be attributable to the higher trans influence of the pentafluorophenyl group compared with the chloro ligand. They are of the same order as found in other similar complexes such as $[AuCl(PFc_2Ph)]$ (2.234(2) Å)[15] for **1** and $[Au(C_6F_5)(PPh_3)]$ (2.265(2) Å)[16] or $[Au_2(\mu\text{-dppf})(C_{16}H_9)_2]$ (2.295(2) Å)[17] for **2**.

Crystal Structures of $[AuL(PPh_2CH_2Fc)]OTf$ (L = PPh_3 (3), $FcCH_2PPh_2$ (5)). Figures 3 and 4 show the crystal structures

Table 2. Selected Bond Lengths (Å) and Angles (deg) for Complex **2**

Au−C(11)	2.070(5)	Au−P	2.284(2)
P−C(21)	1.818(6)	P−C(31)	1.819(5)
P−C(1)	1.828(5)	C(1)−C(41)	1.498(7)
C(11)−Au−P	174.3(2)	C(21)−P−C(31)	105.3(2)
C(21)−P−C(1)	107.3(3)	C(31)−P−C(1)	104.0(2)
C(21)−P−Au	112.1(2)	C(31)−P−Au	116.8(2)
C(1)−P−Au	110.6(2)	C(41)−C(1)−P	111.4(3)

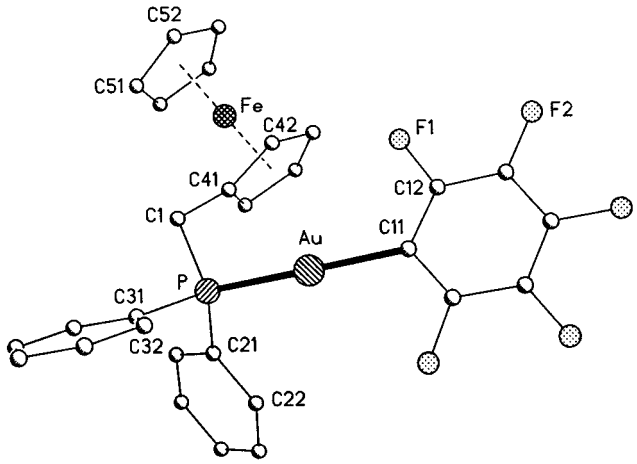

Figure 2. Molecular structure of complex **2** in the crystal. H atoms are omitted for clarity.

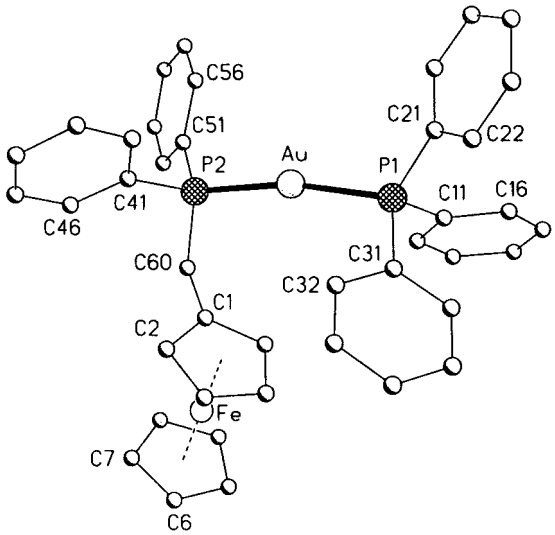

Figure 3. Structure of the cation of complex **3** in the crystal. H atoms are omitted for clarity.

of the cations of **3** and **5**, and Tables 3 and 4 show a selection of bond lengths and angles. The gold atom in complex **3** exhibits a distorted linear geometry with an angle P−Au−P of 168.74(4)°, whereas in **5**, with imposed symmetry, the gold center displays an ideal linear geometry. Deviation from ideal linearity, sometimes by more than 10°, seems to be common for these bis(phosphine) complexes; some examples are $[Au(PFc_2Ph)_2]X$ (X = ClO_4 or PF_6) (169.41(6)°)[18,19] and $[Au\{Fc(CH_2P(CH_2OH)_2\}]Cl$ (176.51(6)°).[10] The Au−P distances are 2.3210(13) and 2.3259(13) Å in **3**, with different phosphine ligands, and 2.309(2) Å in **5**. The latter value is similar to those found in

(18) Gimeno, M. C.; Jones, P. G.; Laguna, A.; Sarroca, C. *J. Organomet. Chem.* **1999**, *579*, 206.
(19) Müller, T. E.; Green, J. C.; Mingos, D. M. P.; MacPartlin, C. M.; Whittingham, C.; Williams, D. J.; Woodroffe, T. M. *J. Organomet. Chem.* **1998**, *551*, 313.

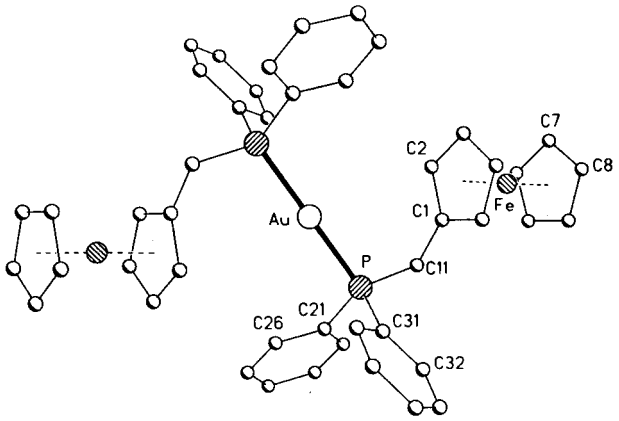

Figure 4. Perspective view of the cation of complex **5** in the crystal. H atoms are omitted for clarity.

Table 3. Selected Bond Lengths (Å) and Angles (deg) for **3**

Au−P(2)	2.3210(13)	Au−P(1)	2.3259(13)
P(1)−C(21)	1.823(4)	P(1)−C(11)	1.824(4)
P(1)−C(31)	1.829(4)	P(2)−C(51)	1.827(4)
P(2)−C(41)	1.831(4)	P(2)−C(60)	1.842(4)
C(1)−C(60)	1.511(6)		
P(2)−Au−P(1)	168.74(4)	C(21)−P(1)−C(11)	104.5(2)
C(21)−P(1)−C(31)	106.2(2)	C(11)−P(1)−C(31)	106.3(2)
C(21)−P(1)−Au	119.66(14)	C(11)−P(1)−Au	110.64(14)
C(31)−P(1)−Au	108.75(14)	C(51)−P(2)−C(41)	106.0(2)
C(51)−P(2)−C(60)	105.4(2)	C(41)−P(2)−C(60)	107.1(2)
C(51)−P(2)−Au	116.42(14)	C(41)−P(2)−Au	113.2(2)
C(60)−P(2)−Au	108.2(2)	C(12)−C(11)−P(1)	118.9(3)
C(16)−C(11)−P(1)	121.3(3)	C(22)−C(21)−P(1)	121.3(3)
C(26)−C(21)−P(1)	119.7(3)	C(36)−C(31)−P(1)	121.7(3)
C(32)−C(31)−P(1)	118.4(3)	C(42)−C(41)−P(2)	120.5(3)
C(46)−C(41)−P(2)	120.7(3)	C(52)−C(51)−P(2)	122.1(3)
C(56)−C(51)−P(2)	118.6(3)	C(1)−C(60)−P(2)	111.3(3)

Table 4. Selected Bond Lengths (Å) and Angles (deg) for Complex **5**

Au−P#1[a]	2.309(2)	P−C(11)	1.825(8)
P−C(21)	1.819(8)	C(1)−C(11)	1.484(10)
P−C(31)	1.820(8)		
P#1−Au−P	180.00(5)	C(21)−P−Au	111.6(2)
C(21)−P−C(31)	105.6(3)	C(31)−P−Au	111.3(2)
C(21)−P−C(11)	107.9(3)	C(11)−P−Au	111.7(3)
C(31)−P−C(11)	108.5(3)		

[a] Symmetry transformations used to generate equivalent atoms: (#1) $-x, -y + 1, -z$.

the complex $[Au(PFc_2Ph)_2]ClO_4$ (2.293(2) and 2.301(2) Å), whereas the former are more similar to those in alkyl or aryl phosphine complexes such as $[Au(PR_3)_2]^+$ ($PR_3 = PPh_2Me$, 2.316(4) Å; PCy_3, 2.321(2) Å).[20,21]

Crystal Structure of $[Au(C_6F_5)_3(PPh_2CH_2Fc)]$ (7). The molecular structure of complex **7** is shown in Figure 5, with selected bond lengths and angles in Table 5. The gold center exhibits the expected square planar coordination, lying 0.015(1) Å out of the ligand plane. The Au−C distances are in the range 2.067(3)−2.080(4) Å and are similar to those found in other tris(pentafluorophenyl)gold(III) derivatives.[22] The Au−P distance (2.3503(9) Å) compares well with the longest found in phosphinogold(III) complexes such as $NBu_4[\{Au(C_6F_5)_3PPh_2CH_2PPh_2\}_2Au]$[23] (2.367(2) Å) and $[AuMe_3(PPh_3)]$[24] (2.350(6) Å and 2.347(6) Å, two independent molecules), but longer than in $[AuCl_3(PPh_3)]$[25] (2.335(4) Å) or $[Au(C_6F_5)(S_2C_6H_4)(PPh_3)]$[26] (2.340(1) Å), consistent with the higher trans influence of the pentafluorophenyl groups.

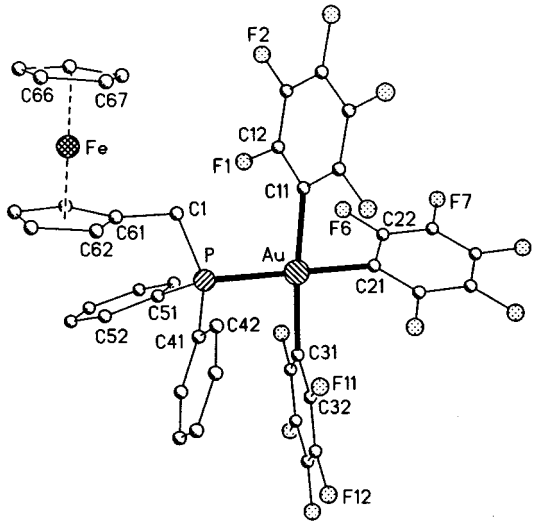

Figure 5. Molecular structure of complex **7** in the crystal. H atoms are omitted for clarity.

Table 5. Selected Bond Lengths (Å) and Angles (deg) for **7**

Au−C(21)	2.067(3)	Au−C(11)	2.068(4)
Au−C(31)	2.080(4)	Au−P	2.3503(9)
P−C(41)	1.804(4)	P−C(51)	1.809(4)
P−C(1)	1.835(4)	C(1)−C(61)	1.496(5)
C(21)−Au−C(11)	86.91(13)	C(21)−Au−C(31)	88.59(13)
C(11)−Au−C(31)	174.80(13)	C(21)−Au−P	179.43(11)
C(11)−Au−P	93.30(9)	C(31)−Au−P	91.23(9)
C(41)−P−C(51)	108.9(2)	C(41)−P−C(1)	107.1(2)
C(51)−P−C(1)	105.1(2)	C(41)−P−Au	109.89(12)
C(51)−P−Au	112.69(12)	C(1)−P−Au	112.99(11)
C(61)−C(1)−P	114.9(3)		

Crystal Structure of $[Ag(PPh_2CH_2Fc)_3]OTf$ (10). The structure of the cation of complex **10** is shown in Figure 6, with a selection of bond lengths and angles in Table 6. The silver atom presents a slightly distorted trigonal geometry, lying 0.046 Å out of the plane of the three phosphorus atoms. The Ag−P distances (2.440(4)−2.483(4) Å) are similar to those obtained for three-coordinate silver complexes such as $[AgX(L\text{-}L)]$[27] (L-L = 2,11-bis(diphenylphosphino)methylbenzo[*c*]phenanthrene, X = Cl, $SnCl_3$, ClO_4, or NO_3) (2.40(3)−2.455(1) Å), $[Ag(dppf)(PPh_3)]ClO_4$ (2.4386(13)−2.4870(12) Å)[11b] or to the highest values for $[Ag(7.8\text{-}(PPh_2)_2\text{-}7.8\text{-}C_2B_9H_{10})(PPh_3)]$ (2.3974(10)−2.4942(10) Å)[28] which correspond to the Ag−P(diphosphine) bonds.

Electrochemistry. The electrochemical behavior of these complexes has been studied by cyclic voltammetry at a platinum

(20) Guy, J. J.; Jones, P. G.; Sheldrick, G. M. *Acta Crystallogr.* **1976**, *B32*, 1937.
(21) Muir, J. A.; Muir, M. M.; Pulgar, L. B.; Jones, L. B.; Sheldrick, G. M. *Acta Crystallogr.* **1985**, *C41*, 1174.
(22) Usón, R.; Laguna, A.; Laguna, M.; Castilla, M. L.; Jones, P. G.; Fittschen, C. *J. Chem Soc., Dalton Trans.* **1987**, 3017.
(23) Fernandez, E. J.; Gimeno, M. C.; Jones, P. G.; Laguna, A.; Lopez-de-Luzuriaga, J. M. *Organometallics* **1995**, *14*, 2918.
(24) Stein, J.; Fackler, J. P., Jr.; Paparizos, C.; Chen, H. W. *J. Am. Chem. Soc.* **1981**, *103*, 2192.
(25) Bandali, G.; Clemente, D. A.; Marangoni, G.; Cattalini, L. J. *J. Chem. Soc., Dalton Trans.* **1973**, 886.
(26) Cerrada, E.; Fernandez, E. J.; Gimeno, M. C.; Laguna, A.; Laguna, M.; Terroba, R.; Villacampa, M. D. *J. Organomet. Chem.* **1995**, *492*, 105.
(27) Barrow, M.; Bürgi, H. B.; Camalli, M.; Caruso, F.; Fisher, E.; Venanzi, L. M.; Zambonelli, L. *Inorg. Chem.* **1983**, *22*, 2356.
(28) Crespo, O.; Gimeno, M. C.; Jones, P. G.; Laguna, A. *J. Chem Soc., Dalton Trans.* **1996**, 4583.

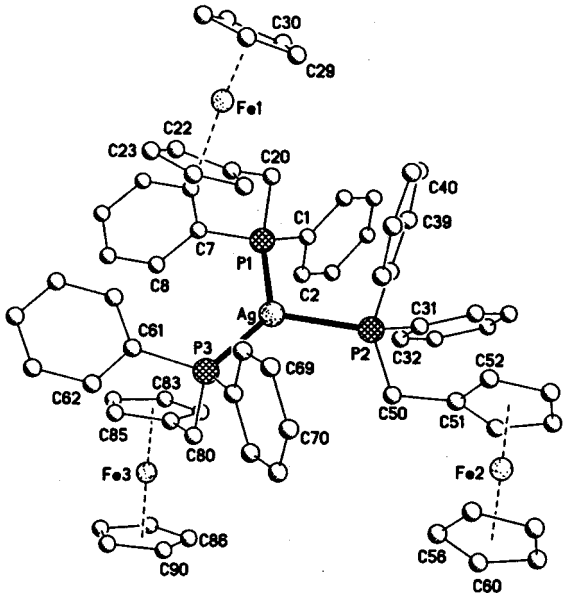

Figure 6. Structure of the cation of complex **10** in the crystal. H atoms are omitted for clarity.

Table 6. Selected Bond Lengths (Å) and Angles (deg) for Complex **10**

Ag−P(1)	2.440(4)	P(2)−C(38)	1.775(12)
Ag−P(3)	2.443(4)	P(2)−C(31)	1.811(9)
Ag−P(2)	2.483(4)	P(2)−C(50)	1.851(15)
P(1)−C(1)	1.822(8)	P(3)−C(67)	1.813(9)
P(1)−C(7)	1.821(8)	P(3)−C(61)	1.825(8)
P(1)−C(20)	1.832(13)	P(3)−C(80)	1.842(14)
P(1)−Ag−P(3)	135.11(14)	C(67)−P(3)−C(80)	106.8(6)
P(1)−Ag−P(2)	112.87(14)	C(61)−P(3)−C(80)	101.6(6)
P(3)−Ag−P(2)	111.32(14)	C(67)−P(3)−Ag	112.9(4)
C(1)−P(1)−C(7)	102.8(5)	C(61)−P(3)−Ag	122.5(3)
C(1)−P(1)−C(20)	104.8(6)	C(80)−P(3)−Ag	108.5(5)
C(7)−P(1)−C(20)	102.3(6)	C(2)−C(1)−P(1)	117.0(6)
C(1)−P(1)−Ag	120.0(4)	C(6)−C(1)−P(1)	123.0(6)
C(7)−P(1)−Ag	119.2(3)	C(8)−C(7)−P(1)	118.5(5)
C(20)−P(1)−Ag	105.6(5)	C(12)−C(7)−P(1)	121.3(5)
C(38)−P(2)−C(31)	105.3(6)	C(21)−C(20)−P(1)	110.6(8)
C(38)−P(2)−C(50)	105.9(7)	C(39)−C(38)−P(2)	121.2(9)
C(31)−P(2)−C(50)	103.8(6)	C(51)−C(50)−P(2)	115.2(10)
C(38)−P(2)−Ag	104.3(5)	C(66)−C(61)−P(3)	118.6(5)
C(31)−P(2)−Ag	117.2(4)	C(68)−C(67)−P(3)	119.3(7)
C(50)−P(2)−Ag	119.0(5)	C(72)−C(67)−P(3)	120.6(7)
C(67)−P(3)−C(61)	103.1(5)	C(81)−C(80)−P(3)	110.7(9)

electrode in CH_2Cl_2. The redox pattern of the free phosphine ligand is complicated and resembles that of the 1,1′-bis-(diphenylphosphino)ferrocene ligand. Thus the phosphine undergoes a quasi-reversible one-electron oxidation process, based on the ferrocene unit, followed by a chemical reaction involving the phosphorus substituent. The cyclic voltammograms, at a scan rate of 100 mV s^{-1}, of the gold derivatives show an essentially reversible wave arising from the oxidation−reduction of the ferrocene moiety at slightly higher potentials than the phosphine−ferrocene ligand. The silver(I) compounds show, in addition to the wave due to the ferrocene oxidation, a more anodic irreversible wave that can be assigned to the one-electron oxidation of Ag^+ to Ag^{2+}. Table 7 summarizes the electrochemical data for these compounds.

Conclusions

We have reported on a series of new gold and silver complexes with ferrocenylmethylphosphine in different coordination numbers. Interesting equilibria or reorganization processes take place in the three-coordinate gold(I) derivatives to give a mixture of the linear, three-coordinate, and four-coordinate species. Several complexes have been characterized by X-ray diffraction; one shows interesting C−H···Cl and H···Au intermolecular contacts that can be considered as weak hydrogen bonds. The electrochemical behavior consists of one reversible electron oxidation process for the gold compounds at slightly higher potential than the ferrocene itself; the silver complexes also show one irreversible wave corresponding to the oxidation to Ag^{2+}.

Table 7. Electrochemical Data for Complexes **1**−**10**

compound	E_1 (V)	E_2 (V)
1 $[AuCl(PPh_2CH_2Fc)]$	0.51	
2 $[Au(C_6F_5)(PPh_2CH_2Fc)]$	0.48	
3 $[Au(PPh_3)(PPh_2CH_2Fc)]OTf$	0.51	
4 $[Ag(PPh_3)(PPh_2CH_2Fc)]OTf$	0.45	1.18
5 $[Au(PPh_2CH_2Fc)_2]ClO_4$	0.53	
6 $[Ag(PPh_2CH_2Fc)_2]OTf$	0.48	1.16
7 $[Au(C_6F_5)_3(PPh_2CH_2Fc)]$	0.56	
8 $[AuCl(PPh_2CH_2Fc)_2]$	0.54	
9 $[Au(PPh_2CH_2Fc)_3]ClO_4$	0.53	
10 $[Ag(PPh_2CH_2Fc)_3]OTf$	0.49	1.1

Experimental Section

Instrumentation. Infrared spectra were recorded in the range 4000−200 cm^{-1} on a Perkin-Elmer 883 spectrophotometer using Nujol mulls between polyethylene sheets. Conductivities were measured in ca. 5×10^{-4} mol dm^{-3} solutions with a Philips 9509 conductimeter. C, H, and S analyses were carried out with a Perkin-Elmer 2400 microanalyzer. Mass spectra were recorded on a VG Autospec, with the liquid secondary-ion mass spectra (LSIMS) technique, using nitrobenzyl alcohol as matrix. NMR spectra were recorded on a Varian Unity 300 spectrometer and a Bruker ARX 300 spectrometer in $CDCl_3$ (otherwise stated). Chemical shifts are cited relative to $SiMe_4$ (^1H, external) and 85% H_3PO_4 (^{31}P, external). Cyclic voltammetric experiments were performed by employing an EG&G PARC model 273 potentiostat. A three-electrode system was used, which consists of a platinum disk working electrode, a platinum wire auxiliary electrode, and a saturated calomel reference electrode. The measurements were carried out in CH_2Cl_2 solutions with 0.1 M Bu_4NPF_6 as a supporting electrolyte. Under the present experimental conditions, the ferrocenium/ferrocene couple was located at 0.47 V vs SCE.

Materials. The starting materials $FcCH_2PPh_2$,[5] $[AuCl(tht)]$,[29] $[Au(C_6F_5)(tht)]$,[30] and $[Au(C_6F_5)_3(OEt_2)]$[31] were prepared by published procedures. $[Au(OTf)(PPh_3)]$ was prepared from $[AuCl(PPh_3)]$[32] by reaction with AgOTf in dichloromethane and $[Ag(OTf)(PPh_3)]$ by reaction of AgOTf and PPh_3 in diethyl ether.

Safety Note. *CAUTION!* Perchlorate salts of metal complexes with organic ligands are potentially explosive. Only small amounts of material should be prepared, and these should be handled with great caution.

Syntheses. [AuR(PPh_2CH_2Fc)] [R = Cl (1), C_6F_5 (2)]. To a solution of $[AuCl(tht)]$ (0.032 g, 0.1 mmol) or $[Au(C_6F_5)(tht)]$ (0.045 g, 0.1 mmol) in 20 mL of dichloromethane was added PPh_2CH_2Fc (0.038 g, 0.1 mmol), and the mixture was stirred for 1 h. Concentration of the solution to ca. 5 mL and addition of hexane (10 mL) gave complexes **1** or **2** as orange solids. Complex **1**: yield 79%. $\Lambda_M = 0.4\ \Omega^{-1}\ cm^2\ mol^{-1}$. Elemental anal. Found: C, 44.87; H, 3.11. Calcd for $C_{23}H_{21}AuClFeP$: C, 44.80; H, 3.43. ^1H NMR, δ: 3.56 (d, 2H, CH_2, J(PH) 10.16 Hz), 4.01 (m, 2H, C_5H_4), 4.04 (m, 2H, C_5H_4), 4.10 (m, 5H, C_5H_5), 7.2−7.6 (m, 10H, Ph). $^{31}P\{^1H\}$ NMR, δ: 30.9 (s). Complex **2**: yield

(29) Usón, R.; Laguna, A. *Organomet. Synth.* **1989**, *3*, 322.
(30) Usón, R.; Laguna, A.; de la Orden, M. U.; Arrese, M. L. *Synth. React. Inorg. Met.-Org. Chem.* **1984**, *14*, 369.
(31) Usón, R.; Laguna, A.; Laguna, M.; Jiménez, J.; Durana, E. *Inorg. Chim. Acta* **1990**, *168*, 89.
(32) Usón, R.; Laguna, A. *Inorg. Synth.* **1982**, *21*, 71.

Table 8. Details of Data Collection and Structure Refinement for the Complexes **1**−**3**

	1	**2**	**3**
chem formula	$C_{23}H_{21}AuClFeP$	$C_{29}H_{21}AuF_5FeP$	$C_{42}H_{36}AuF_3FeO_3P_2S$
cryst habit	yellow block	yellow tablet	orange tablet
cryst size/mm	0.20 × 0.20 × 0.15	0.38 × 0.21 × 0.17	0.68 × 0.48 × 0.16
λ	0.710 73	0.710 73	0.710 73
cryst syst	monoclinic	triclinic	triclinic
space group	$P2_1/c$	$P\bar{1}$	$P\bar{1}$
a/Å	9.886(3)	10.960(2)	10.859(3)
b/Å	17.539(4)	11.049(2)	11.463(4)
c/Å	11.867(3)	12.562(2)	16.517(5)
α/deg		115.374(14)	74.69(2)
β/deg	99.35(2)	109.135(12)	80.33(2)
γ/deg		94.918(14)	79.98(2)
V/Å^3	2030.3(9)	1252.1(4)	1919.1(10)
Z	4	2	2
D_c/g cm^{-3}	2.017	1.985	1.718
M	616.63	748.24	992.52
F(000)	1184	720	980
T/°C	−100	−100	−100
$2\theta_{max}$/deg	50	50	48
μ(Mo $K\alpha$)/cm^{-1}	81.48	65.50	43.87
transmission	0.595−0.801	0.705−0.922	0.610−0.958
no. of reflns meas	5922	4199	6993
no. of unique reflns	3564	4158	5931
R_{int}	0.0393	0.0145	0.014
R^a ($F > 4\sigma(F)$)	0.0328	0.03	0.029
$R_w{}^b$ (F^2, all reflns)	0.0723	0.052	0.072
no. of reflns used	3564	4158	5927
no. of params	244	355	478
no. of restraints	213	93	365
S^c	0.898	0.888	0.996
max $\Delta\rho$/e Å^{-3}	1.271	0.908	2.72

[a] $R(F) = \sum||F_o| - |F_c||/\sum|F_o|$. [b] $R_w(F^2) = [\sum\{w(F_o^2 - F_c^2)^2\}/\sum\{w(F_o^2)^2\}]^{0.5}$; $w^{-1} = \sigma^2(F_o^2) + (aP)^2 + bP$, where $P = [F_o^2 + 2F_c^2]/3$ and a and b are constants adjusted by the program. [c] $S = [\sum\{w(F_o^2 - F_c^2)^2\}/(n - p)]^{0.5}$, where n is the number of data and p the number of parameters.

Table 9. Details of Data Collection and Structure Refinement for the Complexes **5**, **7**, and **10**

	5	**7**	**10**
chem formula	$C_{47}H_{44}AuCl_3Fe_2O_4P_2$	$C_{41}H_{21}AuF_{15}FeP$	$C_{71}H_{65}AgCl_2F_3Fe_3O_3P_3S$
cryst habit	orange plate	orange prism	dull orange tablet
cryst size/mm	0.20 × 0.20 × 0.05	0.50 × 0.40 × 0.20	0.35 × 0.30 × 0.15
cryst system	triclinic	monoclinic	monoclinic
space group	$P\bar{1}$	$P2_1/n$	$P2_1/c$
a/Å	9.0828(18)	13.6515(14)	12.692(3)
b/Å	9.5568(16)	17.101(2)	18.467(4)
c/Å	13.501(2)	16.274(2)	28.693(6)
α/deg	86.587(12)		
β/deg	89.573(14)	91.566(7)	93.08(2)
γ/deg	77.154(14)		
V/Å^3	1140.6(4)	3797.7(6)	6716(3)
Z	1	4	4
D_c/g cm^{-3}	1.674	1.893	1.478
M	1149.18	1082.36	1494.52
F(000)	570	2088	3048
T/°C	−100	−100	−100
$2\theta_{max}$/deg	50	50	46
μ(Mo $K\alpha$)/cm^{-1}	41.24	43.88	11.59
transmission	0.789−0.991	0.608−0.966	
no. of reflns meas	4031	6694	9408
no. of unique reflns	4003	6676	8750
R_{int}	0.038	0.016	0.058
R^a ($F > 4\sigma(F)$)	0.049	0.025	0.095
$R_w{}^b$ (F^2, all reflns)	0.1254	0.044	0.278
no. of reflns used	4003	6676	8750
no. of params	290	532	258
no. of restraints	281	507	19
S^c	0.973	0.886	0.878
max $\Delta\rho$/e Å^{-3}	1.723	0.368	1.252

[a] $R(F) = \sum||F_o| - |F_c||/\sum|F_o|$. [b] $R_w(F^2) = [\sum\{w(F_o^2 - F_c^2)^2\}/\sum\{w(F_o^2)^2\}]^{0.5}$; $w^{-1} = \sigma^2(F_o^2) + (aP)^2 + bP$, where $P = [F_o^2 + 2F_c^2]/3$ and a and b are constants adjusted by the program. [c] $S = [\sum\{w(F_o^2 - F_c^2)^2\}/(n - p)]^{0.5}$, where n is the number of data and p the number of parameters.

85%. $\Lambda_M = 1.7\ \Omega^{-1}$ cm^2 mol^{-1}. Elemental anal. Found: C, 46.73; H, 3.22. Calcd for $C_{29}H_{21}AuF_5FeP$: C, 46.55; H, 2.83. ^{1}H NMR, δ: 3.58 (d, 2H, CH_2, J(PH) 9.43 Hz), 4.05 (m, 2H, C_5H_4), 4.08 (m, 2H, C_5H_4), 4.10 (m, 5H, C_5H_5), 7.2−7.7 (m, 10H, Ph). ^{31}P{^{1}H} NMR, δ: 30.1 (m).

^{19}F NMR, δ: −116.3 (m, 2F, *o*-F), −158.8 (t, 1F, *p*-F, *J*(FF) 20.0 Hz), −162.7 (m, 2F, *m*-F).

[M(PPh$_2$CH$_2$Fc)(PPh$_3$)]OTf [M = Au (3), Ag (4)]. To a solution of [Au(OTf)(PPh$_3$)] (0.061 g, 0.1 mmol) or [Ag(OTf)(PPh$_3$)] (0.052 g, 0.1 mmol) in 20 mL of dichloromethane was added PPh_2CH_2Fc (0.038 g, 0.1 mmol), and the mixture was stirred for 1 h. Concentration of the solution to ca. 5 mL and addition of hexane (10 mL) gave **3** or **4** as yellow solids. Complex **3**: yield 95%. Λ_M = 105 Ω^{-1} cm^2 mol^{-1}. Elemental anal. Found: C, 50.39; H, 3.31; S, 3.31. Calcd for $C_{42}H_{36}AuF_3FeO_3P_2S$: C, 50.82; H, 3.65; S, 3.23. ^1H NMR, δ: 3.82 (m, 1H, CH_2), 3.90 (m, 1H, CH_2), 3.93 (m, 2H, C_5H_4), 3.95 (m, 2H, C_5H_4), 4.12 (m, 5H, C_5H_5), 4.14 (s, 5H, C_5H_5), 7.2−7.7 (m, 25H, Ph). $^{31}P\{^1H\}$ NMR, δ: 44.4 (s), 45.3 (s). Complex **4**: yield 65%. Λ_M = 104.2 Ω^{-1} cm^2 mol^{-1}. Elemental anal. Found: C, 55.95; H, 3.79; S, 3.33. Calcd for $C_{42}H_{36}AgF_3FeO_3P_2S$: C, 55.78; H, 4.01; S, 3.54. ^1H NMR, −80 °C, $(CD_3)_2CO$, δ: 3.55 (m, 2H, CH_2), 3.80 (m, 2H, C_5H_4), 3.94 (m, 2H, C_5H_4), 4.06 (m, 5H, C_5H_5), 7.2−7.7 (m, 25H, Ph). $^{31}P\{^1H\}$ NMR, δ: P_A 12.4, P_B 15.8, *J*(P_AP_B) 45 Hz, *J*($P_A{}^{107}$Ag) 375 Hz, *J*($P_A{}^{109}$Ag) 427.5 Hz, *J*($P_B{}^{107}$Ag) 500 Hz, *J*($P_B{}^{109}$Ag) 570 Hz.

[M(PPh$_2$CH$_2$Fc)$_2$]X [M = Au, X = ClO$_4$ (5); Ag, X = OTf (6)]. To a solution of $[Au(tht)_2]ClO_4$ (0.047 g, 0.1 mmol) or AgOTf (0.021 g, 0.1 mmol) in 20 mL of dichloromethane was added PPh_2CH_2Fc (0.076 g, 0.2 mmol), and the mixture was stirred for 1 h. Concentration of the solution to ca. 5 mL and addition of hexane (10 mL) gave **5** or **6** as yellow solids. Complex **5**: yield 93%. Λ_M = 100 Ω^{-1} cm^2 mol^{-1}. Elemental anal. Found: C, 51.61; H, 3.73. Calcd for $C_{46}H_{42}AuClFe_2O_4P_2$: C, 51.88; H, 3.97. ^1H NMR, δ: 3.86 (m, 2H, CH_2), 3.94 (m, 2H, C_5H_4), 3.98 (m, 2H, C_5H_4), 4.17 (m, 5H, C_5H_5), 7.4−7.8 (m, 20H, Ph). $^{31}P\{^1H\}$ NMR, δ: 44.2 (s). Complex **6**: yield 65%. Λ_M = 115 Ω^{-1} cm^2 mol^{-1}. Elemental anal. Found: C, 55.62; H, 4.39; S, 2.74. Calcd for $C_{47}H_{42}AgF_3Fe_2O_3P_2S$: C, 55.05; H, 4.13; S, 3.12. ^1H NMR, δ: 3.26 (m, 2H, CH_2), 3.72 (m, 2H, C_5H_4), 3.84 (m, 2H, C_5H_4), 4.03 (m, 5H, C_5H_5), 7.1−7.5 (m, 20H, Ph). $^{31}P\{^1H\}$ NMR, −60 °C $CDCl_3$, δ: 8.6 ppm (2d, *J*(P^{107}Ag) 320 Hz, *J*(P^{109}Ag) 367.8 Hz).

[Au(C$_6$F$_5$)$_3$(PPh$_2$CH$_2$Fc)] (7). To a solution of $[Au(C_6F_5)_3(OEt_2)]$ (0.077 g, 0.1 mmol) in 20 mL of dichloromethane was added PPh_2CH_2Fc (0.038 g, 0.1 mmol), and the mixture was stirred for 1 h. Concentration of the solution to ca. 5 mL and addition of hexane (10 mL) gave complex **7** as an orange solid. Yield: 91%. Λ_M = 0.4 Ω^{-1} cm^2 mol^{-1}. Elemental anal. Found: C, 45.68; H, 1.72. Calcd for $C_{41}H_{21}AuF_{15}FeP$: C, 45.49; H, 1.95. ^1H NMR, δ: 3.47 (d, 2H, CH_2, *J*(PH) 7.87 Hz), 3.74 (m, 2H, C_5H_4), 3.99 (m, 2H, C_5H_4), 4.04 (m, 5H, C_5H_5), 7.2−7.7 (m, 10H, Ph). $^{31}P\{^1H\}$ NMR, δ: 13.9 (m). ^{19}F NMR, δ: −120.1 (m, 4F, *o*-F), −121.8 (m, 2F, *o*-F), −156.9 (t, 2F, *p*-F, *J*(FF) 19.75 Hz), −157.4 (t, 1F, *p*-F, *J*(FF) 19.88 Hz), −160.7 (m, 4F, *m*-F), −161.4 (m, 2F, *m*-F).

[AuCl(PPh$_2$CH$_2$Fc)$_2$] (8). To a solution of [AuCl(tht)] (0.032 g, 0.1 mmol) in 20 mL of dichloromethane was added PPh_2CH_2Fc (0.076 g, 0.2 mmol), and the mixture was stirred for 1 h. Concentration of the solution to ca. 5 mL and addition of hexane (10 mL) gave **8** as an orange solid. Complex **8**: yield 50%. Λ_M = 14 Ω^{-1} cm^2 mol^{-1}. Elemental anal. Found: C, 55.73; H, 3.71. Calcd for $C_{46}H_{42}AuClFe_2P_2$: C, 55.31; H, 4.03. ^1H NMR, CD_2Cl_2, room temperature, δ: 3.69 (d, 2H, CH_2, *J*(PH) 9.6 Hz), 4.04 (m, 2H, C_5H_4), 4.05 (m, 2H, C_5H_4), 4.14 (m, 5H, C_5H_5), 7.4−7.7 (m, 20H, Ph). $^{31}P\{^1H\}$ NMR, δ: 33.8 (s, br); −80 °C, 3.60 (d, 2H, CH_2, *J*(PH) 10.5 Hz), 3.79 (m, C_5H_4), 3.95 (m, C_5H_4), 3.99 (m, C_5H_4), 4.01 (m, C_5H_4), 4.08 (m, C_5H_5), 7.4−7.7 (m, Ph). $^{31}P\{^1H\}$ NMR, δ: 28.2 (s), 32.4 (s), 38.5(s), 42.3 (s).

[M(PPh$_2$CH$_2$Fc)$_3$]X [M = Au, X = ClO$_4$ (9); M = Ag, X = OTf (10)]. To a solution of $[Au(tht)_2]ClO_4$ (0.047 g, 0.1 mmol) or AgOTf (0.021 g, 0.1 mmol) in 20 mL of dichloromethane was added PPh_2CH_2Fc (0.114 g, 0.3 mmol), and the mixture was stirred for 1 h. Concentration of the solution to ca. 5 mL and addition of hexane (10 mL) gave **9** or **10** as yellow solids. Complex **9**: yield 80%. Λ_M = 90.5 Ω^{-1} cm^2 mol^{-1}. Elemental anal. Found: C, 57.42; H, 3.92. Calcd for $C_{69}H_{63}AuClFe_3O_4P_3$: C, 57.19; H, 4.38. ^1H NMR, room temperature, δ: 3.77 (m, 6H, CH_2), 3.94 (m, 12H, C_5H_4), 4.15 (m, 15H, C_5H_5), 7.2−7.8 (m, 30H, Ph). $^{31}P\{^1H\}$ NMR, δ: 41.7 (s, br); −60 °C, 3.77 (m), 3.84 (m), 3.97 (m), 4.10 (m), 7−7.8 (m, Ph). $^{31}P\{^1H\}$ NMR, δ: 28.2 (s), 38.3 (s), 43.8 (s). Complex **10**: yield 85%. Λ_M = 107 Ω^{-1} cm^2 mol^{-1}. Elemental anal. Found: C, 59.7; H, 3.91; S, 2.82. Calcd for $C_{70}H_{63}AgF_3Fe_3O_3P_3S$: C, 59.38; H, 4.40; S, 2.29. ^1H NMR, δ: 3.37 (m, 2H, CH_2), 3.81 (m, 2H, C_5H_4), 3.83 (m, 2H, C_5H_4), 4.05 (m, 5H, C_5H_5), 7.3−7.5 (m, 30H, Ph). $^{31}P\{^1H\}$ NMR, −60 °C, δ: 14.8 ppm (2d,
J(P^{107}Ag) 509 Hz, *J*(P^{109}Ag) 586.3 Hz).

Crystallography. The crystals were mounted in inert oil on a glass fiber and transferred to the cold gas stream of a Siemens P4 diffractometer equipped with an LT-2 or Oxford low-temperature attachment. Data were collected using monochromated Mo Kα radiation (λ = 0.710 73 Å). Scan type: ω or $\theta-2\theta$ (**3**). Cell constants were refined from setting angles of ca. 60 reflections in the range 2θ 7−25°. Psi scans were applied for all of the complexes with the exception of compound **10**, for which no absorption correction was applied. The structures were solved by direct methods for **3** and **10**, otherwise by the heavy-atom method, and refined on F^2 using the programs SHELXL-93 or SHELXL-97.[33] All non-hydrogen atoms were refined anisotropically (except for complex **10**). Hydrogen atoms were included using a riding model. Special refinement details: A system of restraints to light-atom displacement-factor components and local ring symmetry was used. Compounds **3** and **10** contain badly disordered solvent (dichloromethane). Further details of the data collection are given in Tables 8 and 9.

Acknowledgment. We thank the Dirección General de Investigación Científica y Técnica (No. PB97-1010-C02-01), the Caja de Ahorros de la Inmaculada (No. CB4/98), and the Fonds der Chemischen Industrie for financial support.

Supporting Information Available: Six X-ray crystallographic files, in CIF format. This material is available free of charge via the Internet at http://pubs.acs.org.

IC9905446

(33) Sheldrick, G. M. *SHELXL-93 and SHELXL-97, Program for Crystal Structure Refinement*; University of Göttingen: Göttingen, Germany, 1993/1997.